

## Design, Synthesis and X-ray Structure of Protein–Ligand Complexes: Important Insight into Selectivity of Memapsin 2 ( $\beta$ -Secretase) Inhibitors

Arun K. Ghosh,<sup>\*,†</sup> Nagaswamy Kumaragurubaran,<sup>†</sup> Lin Hong,<sup>‡,§</sup> Hui Lei,<sup>‡</sup> Khaja Azhar Hussain,<sup>§</sup> Chun-Feng Liu,<sup>‡</sup> Thippeswamy Devasamudram,<sup>‡</sup> Vajira Weerasena,<sup>‡</sup> Robert Turner,<sup>‡</sup> Gerald Koelsch,<sup>‡,§</sup> Geoffrey Bilcer,<sup>‡</sup> and Jordan Tang<sup>§,⊥</sup>

Departments of Chemistry and Medicinal Chemistry, Purdue University, West Lafayette, Indiana 47907, Zapaq Inc., Oklahoma City, Oklahoma 73104, Protein Studies Program, Oklahoma Medical Research Foundation and Department of Biochemistry and Molecular Biology, University of Oklahoma Health Science Center, Oklahoma City, Oklahoma 73104

Received December 20, 2005; E-mail: akghosh@purdue.edu

The proteolytic enzyme memapsin 2 ( $\beta$ -secretase, BACE-1) has emerged as a leading target for therapeutic intervention of Alzheimer's disease (AD).<sup>1</sup> It is one of two proteases that cleave the  $\beta$ -amyloid precursor protein (APP) to generate the 40/42 residue amyloid- $\beta$  peptide (A $\beta$ ). The excess level of A $\beta$  leads to formation of amyloid plaques and neurofibrillary tangles in the brain.<sup>2,3</sup> The neurotoxicity of A $\beta$  eventually leads to the death of neurons, inflammation of the brain, dementia, and AD.<sup>4</sup> On the basis of initial kinetics and substrate specificity data,<sup>5</sup> we designed a number of potent inhibitors incorporating a nonhydrolyzable Leu-Ala hydroxyethylene dipeptide isostere.<sup>6</sup> One such inhibitor is OM99-2 (**1**, Figure 1) which has a  $K_i$  value of 1.6 nM for human memapsin 2.<sup>6a</sup> An X-ray crystal structure of **1**-bound memapsin 2 was determined at 1.9 Å resolution.<sup>7</sup> The structure provided molecular insight into the ligand–binding site interactions of the memapsin 2 active site.

Subsequently, our preliminary structure–activity relationship studies led to the design of potent peptidomimetic inhibitor **2** with a  $K_i$  value of 2.5 nM against memapsin 2.<sup>6b</sup> However, it displayed no selectivity over memapsin 1 (BACE-2) or cathepsin D. From a therapeutic point of view, the selectivity of memapsin 2 inhibitors over other human aspartic proteases is expected to be important, especially memapsin 1 and cathepsin D.

Memapsin 1, which has specificity similarity with memapsin 2,<sup>8</sup> has independent physiological functions. Cathepsin D, which is abundant in all cells, plays an important role in cellular protein catabolism.<sup>9</sup> Its inhibition would likely consume inhibitor drugs as well as lead to probable toxicity.

The X-ray structure of **1**-bound memapsin 2 revealed a number of critical ligand-binding site interactions in the S<sub>2</sub>- and S<sub>3</sub>-subsites.<sup>7</sup> Based upon examination of this X-ray structure and a model of memapsin 1, it appears that the residues in the S<sub>2</sub>- and S<sub>3</sub>-subsites may be suitable for building selectivity over memapsin 1 and cathepsin D. Herein we report our structure-based design of novel memapsin 2 inhibitors that incorporate methylsulfonyl alanine as the P<sub>2</sub>-ligand and pyrazole and oxazole-derived heterocycles as the P<sub>3</sub>-ligands (see Figure 2). The corresponding inhibitors have exhibited enhanced potency against memapsin 2 and excellent selectivity over memapsin 1 and cathepsin D. Furthermore, the protein–ligand X-ray structure of the pyrazole-bearing inhibitor provided important molecular insight into the specific cooperative ligand–binding site interactions for selectivity design.

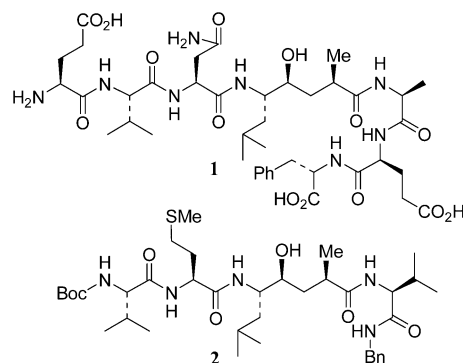


Figure 1. Structure of Inhibitors **1** and **2**.

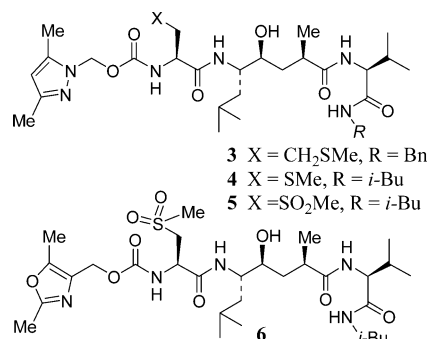


Figure 2. Structure of Inhibitors **3**–**6**.

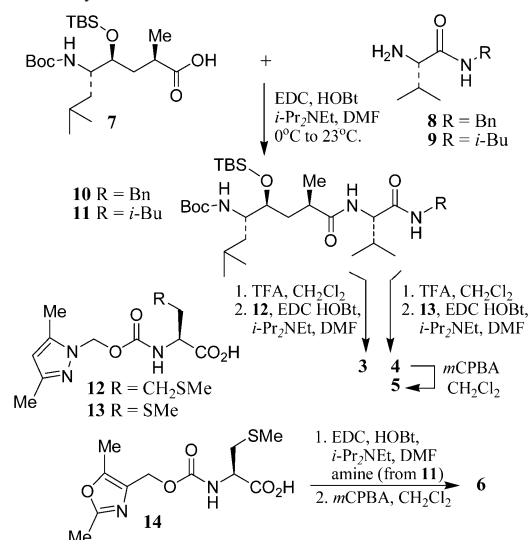
The synthesis of inhibitors **3**–**6** is outlined in Scheme 1. Coupling of previously described<sup>6</sup> Leu-Ala dipeptide isostere **7** with valine derivatives **8** and **9** using EDC and HOBt in the presence of *i*-Pr<sub>2</sub>NEt provided derivatives **10** and **11** (71–95%). Urethanes **12** and **13** were prepared by treatment of 2,5-dimethylpyrazolylmethanol with triphosgene in CH<sub>2</sub>Cl<sub>2</sub> followed by addition of methionine and methylcysteine methyl esters to provide the corresponding urethanes.<sup>10</sup> Saponification of the resulting methyl esters with aqueous lithium hydroxide provided **12** and **13** (36–44%). Removal of Boc and TBS groups by exposure of **10** and **11** to trifluoroacetic acid and coupling of the resulting amines with the corresponding acids using EDC and HOBt afforded inhibitors **3** and **4** (40–64%). Oxidation of sulfide **4** with *m*CPBA in a mixture (6:1) of CH<sub>2</sub>Cl<sub>2</sub> and MeOH furnished sulfone **5** (86%). Acid **14** was prepared by alkoxycarbonylation<sup>10</sup> of 2,5-dimethyl-4-oxazolmethanol<sup>11</sup> and methylcysteine methyl ester followed by saponification of the resulting ester (see Supporting Information for details). It was converted to inhibitor **6** by analogous procedures described above.

<sup>†</sup> Purdue University.

<sup>‡</sup> Zapaq Inc.

<sup>§</sup> Oklahoma Medical Research Foundation and <sup>⊥</sup>Department of Biochemistry and Molecular Biology, University of Oklahoma Health Science Center.

<sup>‡</sup>Department of Biochemistry and Molecular Biology, University of Oklahoma Health Science Center.

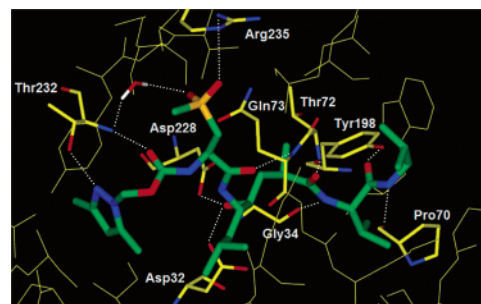
**Scheme 1.** Synthesis of Inhibitors 3–6**Table 1.**  $K_i$  Values and Selectivities for Inhibitors 2–6<sup>a</sup>

compd	M2 (nM)	M1 (nM)	CD (nM)	selectivity ratios		IC <sub>50</sub> (μM)
				M1/M2	CD/M2	
2	2.5	1.2	nd	—	—	6.5
3	14	811	25	58	1.8	nd
4	4.4	161	15	36	3	nd
5	0.3	356	131	1186	436	1.4
6	0.12	458	304	>3800	>2500	1.7

<sup>a</sup> Data represent the mean value of 3–5 determinations; memapsin 2 (M2), memapsin 1 (M1), cathepsin D (CD); nd, not determined.

Potencies of various inhibitors were determined against recombinant memapsin 2, memapsin 1, and human cathepsin D. The results are shown in Table 1. As shown, inhibitor **2** with P<sub>3</sub>-Boc-Val is more potent for memapsin 1 than memapsin 2. Incorporation of pyrazolymethyl urethane in place of P<sub>3</sub>-Boc-Val provided inhibitor **3** having a >5-fold reduction in potency for memapsin 2 compared to inhibitor **2**. Inhibitor **3** also showed significantly reduced activity against M1 with a  $K_i$  value of 811 nM (58-fold selectivity over M1) but showed little selectivity for M2 over CD. Inhibitor **4** with a P<sub>3</sub>'-isobutylamide and P<sub>2</sub>-methylcysteine has shown a 3-fold enhancement of M2 potency. It has also shown >36-fold selectivity over M1 and a modest 3-fold selectivity over CD. Based upon inhibitor models, the P<sub>2</sub>-methionine in **3** or P<sub>2</sub>-methylcysteine side chain in **4** does not appear to be forming a hydrogen bond with Arg-235 of memapsin 2. However, the corresponding P<sub>2</sub>-sulfone of **4** appears to be in close proximity to Arg-235 of memapsin 2. Indeed, oxidation of the P<sub>2</sub>-methyl cysteine provided inhibitor **5** (MW 658) with very impressive potency (M<sub>2</sub>  $K_i$  0.3 nM) and selectivity for memapsin 2. It displayed 1186-fold selectivity over M1 and 436-fold selectivity over CD.

To gain further molecular insight, the **5**-bound memapsin 2 X-ray structure was determined at 1.8 Å resolution (Figure 3).<sup>12</sup> As it appears from the structure, one of the P<sub>3</sub>-pyrazole nitrogens is within hydrogen-bonding distance to Thr-232 with one of the dimethyl groups effectively filling in the shallow hydrophobic pocket in the S<sub>3</sub>-subsite and the other occupying the hydrophobic S<sub>3</sub>-site. In addition, the P<sub>2</sub>-sulfone functionality is within hydrogen-bonding distance to Arg-235 as well as with a tightly bound water molecule in the S<sub>2</sub>-site. These interactions of the P<sub>2</sub> and P<sub>3</sub> ligands are presumably responsible for the observed enhanced selectivity for inhibitor **5** compared to that for inhibitor **4**.

**Figure 3.** Inhibitor-5-bound X-ray structure of memapsin 2.

On the basis of this molecular insight into the selectivity, we designed the oxazolymethyl P<sub>3</sub>-ligand for inhibitor **6** (MW 659). This provided by far the most potent (M<sub>2</sub>  $K_i$  0.12 nM) and selective inhibitor (>3800-fold over M1 and >2500-fold over CD). We have also determined the cellular inhibition of memapsin 2 by inhibitors **5** and **6** in Chinese hamster ovary cells. They have shown an average cellular IC<sub>50</sub> value of 1.4 and 1.7 μM respectively, compared to an IC<sub>50</sub> value of 45 μM for **1**.<sup>13</sup>

In conclusion, our structure-based design led to the development of very potent and highly selective memapsin 2 inhibitors. Furthermore, our X-ray structural analysis of protein–inhibitor complexes has uncovered potentially important molecular interactions useful in the design of selectivity against other aspartyl proteases. Additional studies to further elucidate the role of these and other interactions important for selectivity are in progress.

**Acknowledgment.** Financial support by the National Institutes of Health (AG 18933) is gratefully acknowledged.

**Supporting Information Available:** Experimental procedures and spectral data for **3–6**, **10–14**, and X-ray information and complete ref 3a. This material is available free of charge via the Internet at <http://pubs.acs.org>.

## References

- Vassar, R.; Citron, M. *Neuron* **2000**, *27*, 419.
- (a) Roggo, A. *Curr. Top. Med. Chem.* **2002**, *2*, 359. (b) Olson, R. E.; Thompson, L. A. *Ann. Rep. Med. Chem.* **2000**, *35*, 31.
- (a) Vassar, R. et al. *Science* **1999**, *286*, 735. (b) Lin, X.; Koelsch, G.; Wu, S.; Downs, D.; Dashti, A.; Tang, J. *Proc. Natl. Acad. Sci. U.S.A.* **2000**, *97*, 1456. (c) Sinha, S.; Lieberburg, I. *Proc. Natl. Acad. Sci. U.S.A.* **1999**, *96*, 11049.
- (a) Selkoe, D. J. *Nature* **1999**, *399A*, 23. (b) Selkoe, D. *Physiol. Rev.* **2001**, *81*, 741.
- Turner, R.; Koelsch, G.; Hong, L.; Castenheira, P.; Ghosh, A. K.; Tang, J. *Biochemistry* **2001**, *40*, 10001.
- (a) Ghosh, A. K.; Shin, D.; Downs, D.; Koelsch, G.; Lin, X.; Ermolieff, J.; Tang, J. *J. Am. Chem. Soc.* **2000**, *122*, 3522. (b) Ghosh, A. K.; Bilcer, G.; Harwood, C.; Kawahama, R.; Shin, D.; Downs, D.; Hussain, K. A.; Hong, L.; Loy, J. A.; Nguyen, C.; Koelsch, G.; Ermolieff, J.; Tang, J. *J. Med. Chem.* **2001**, *44*, 2865.
- Hong, L.; Koelsch, G.; Lin, X.; Wu, S.; Terzyan, S.; Ghosh, A. K.; Zhang, X. C.; Tang, J. *Science* **2000**, *290*, 150.
- Turner, R. T.; Loy, J. A.; Nguyen, C.; Devasamudram, T.; Ghosh, A. K.; Koelsch, G.; Tang, J. *Biochemistry* **2002**, *41*, 8742.
- Diment, S.; Leech, M. S.; Stahl, P. D. *J. Biol. Chem.* **1988**, *263*, 6901.
- Ghosh, A. K.; Duong, T. T.; McKee, S. P.; Thompson, W. J. *Tetrahedron Lett.* **1992**, *33*, 2781.
- Kukla, M. J.; Fortunato, J. M. *J. Org. Chem.* **1984**, *49*, 5003.
- The protein–ligand X-ray structure of **5**-bound memapsin 2 has been deposited in PDB (PDB ID: 2G94). For a stereoview and crystallographic information, please see Supporting Information.
- Chang, W. P.; Koelsch, G.; Wong, S.; Downs, D.; Da, H.; Weerasena, V.; Gordon, B.; Devasamudram, T.; Bilcer, G.; Ghosh, A. K.; Tang, J. *J. Neurochem.* **2004**, *89*, 1409.

JA058636J